

How *Comamonas testosteroni* and *Rhodococcus ruber* enhance nitrification in the presence of quinoline

Ge Zhu^a, Haiyun Zhang^a, Ru Yuan^a, Meng Huang^a, Fei Liu^a, Mo Li^{a,**}, Yongming Zhang^{a,*}, Bruce E. Rittmann^b

^a Department of Environmental Engineering, School of Environmental and Geographical Sciences, Shanghai Normal University, Shanghai, 200234, P.R. China

^b Biodesign Swette Center for Environmental Biotechnology, Arizona State University, Tempe, AZ85287-5701, United States

ARTICLE INFO

Keywords:

Nitrification
Nitrifier
Quinoline
Bio-inhibition
Biodegradation

ABSTRACT

Because many wastewater-treatment plants receive effluents containing inhibitory compounds from chemical or pharmaceutical facilities, the input of these inhibitors can lead to failure of nitrification and total-N removal. Nitrification *de facto* is the more important process, as it is the first step of nitrogen removal and involves slow-growing autotrophic bacteria. In this work, quinoline, the target compound severely inhibited nitrification: The biomass-normalized nitrification rate decreased four-fold in the presence of quinoline. The inhibition was relieved by bioaugmenting *Comamonas testosteroni* or *Rhodococcus ruber* to the nitrifying biomass. Because the inhibition was derived from a quinoline intermediate, 2-hydroxyl quinoline (2HQ), not quinoline itself, nitrification was accelerated only after 2HQ disappeared due to the addition of *R. ruber* or *C. testosteroni*. *R. ruber* was superior to *C. testosteroni* for 2HQ biodegradation and accelerating nitrification. Besides accelerating nitrification, adding *C. testosteroni* or *R. ruber* led to the enrichment of *Nitrospira*, which appeared to be carrying out commammox metabolism, since ammonium-oxidizing bacteria were not enriched.

1. Introduction

Nitrogen removal, a pressing topic in wastewater treatment (Yu et al., 2022a; Oliveira et al., 2021), usually is realized by combining nitrification and denitrification. Nitrification *de facto* is the more important process, as it is the first step of nitrogen removal and involves slow-growing autotrophic bacteria (Rittmann and McCarty, 2020; Sterngren et al., 2020; Chaali et al., 2021; Drewnowski et al., 2021). In addition, nitrifying bacteria are sensitive to inhibition from recalcitrant organic compounds, with the inhibition inactivating or further slowing the growth of the nitrifiers (Suszek-Opatka et al., 2016; Rochmah et al., 2020). Because many wastewater-treatment plants (WWTPs) receive effluents containing inhibitory compounds from chemical or pharmaceutical facilities, the input of these un-pretreated wastewaters can lead to failure of nitrification and total-N removal. (Deng et al., 2017; Tong et al., 2019; Zhang et al., 2021).

It is difficult to recover nitrification activity quickly, because the nitrifiers grow slowly (Rittmann and McCarty, 2020). A strategy to accelerate the resumption of nitrification activity is to replace damaged

sludge with biomass that is acclimated to the toxicants (Zou et al., 2019). Even better would be to acclimate the biomass to the toxicants on a routine basis (Zou et al., 2020; Zhang et al., 2021). Both strategies have been successfully applied for recovering the activity of activated sludge damaged from inputs of phenol, 2,4,6-trichlorophenol (2,4,6-TCP) and *para*-nitrophenol (PNP) (Zou et al., 2019, 2020; Zhang et al., 2021). Activated sludge acclimated to phenol, 2,4,6-TCP, and PNP protected the nitrifiers by relieving toxicity from the three toxicants.

Despite success in the prior studies, many questions remain to be resolved. For example, was the input organic molecule or one of its biodegradation intermediates the main inhibitor of the nitrifiers? Are specific bacterial strains (out of the entire community of the acclimated activated sludge) especially effective at relieving inhibition? In particular, if a specific strain were the dominant source of detoxification, cultivating it may be less costly than maintaining an entire culture of acclimated biomass.

Here, we target quinoline, a nitrogenous heterocyclic compound, to investigate how it inhibits nitrifiers and how isolated heterotrophic bacteria can relieve the inhibition. Quinoline is used in the synthesis of

* Corresponding author.

** Co-corresponding author.

E-mail addresses: leemotto@shnu.edu.cn (M. Li), zhym@shnu.edu.cn (Y. Zhang).

drugs and dyes, as well as solvents and analytical reagent (Felczak et al., 2016; Zhu et al., 2021b). Quinoline also is one of the main components in coking wastewater (Xu et al., 2017), which might be discharged into municipal sewers and reach WWTPs (Lyu et al., 2020). Full quinoline biodegradation or mineralization requires a series of steps, and the first two steps usually are mono-oxygenation reactions (Bai et al., 2015; Zhu et al., 2021a). Fig. S1 in Supplementary Information shows the full biotransformation and mineralization pathway for quinoline, and 2-hydroxyl quinoline (2HQ) is the main intermediate of quinoline mono-oxygenation (Bai et al., 2015). 2HQ also is used as a pharmaceutical feedstock, which suggests that 2HQ could exhibit inhibition to microorganisms. What we do not know is if quinoline or 2HQ plays the main role of inhibiting nitrifying bacteria.

We utilized two strains of heterotrophic bacteria that were isolated from quinoline-acclimated activated sludge based on their ability to biodegrade quinoline (Zhu et al., 2021a, 2021b). In this work, we used them for accelerating nitrification by relieving inhibition. We specifically investigated how the heterotrophic bacteria relieved inhibition to nitrification, include whether quinoline or 2HQ was the dominant inhibitor.

2. Materials and method

2.1. Chemicals and media preparation

All chemicals were purchased from TITAN Technology Co., Ltd. in Shanghai. A volume of 3.55 mL of pure quinoline liquid was diluted into 1 L of deionized water to obtain a quinoline stock solution of 30 mM. A 2-hydroxyl quinoline (2HQ) stock solution was prepared by diluting 29 mg 2HQ in 1 L.

The trace-element solution was prepared as in Zhu et al. (2021a, 2021b). The mineral salts medium contained 0.25 g NaH₂PO₄, 0.75 g K₂HPO₄, 0.2 g MgSO₄·7H₂O, 0.006 g CaCl₂, 0.001 g FeSO₄·7H₂O, and 2 mL trace-element solution were diluted in 1 L deionized water; the medium was sterilized at 121 °C and 0.10 ~ 0.15 MPa for 20 min.

The ammonium chloride stock solution was prepared by diluting 30.8 g ammonium chloride in 1 L deionized water (0.58 M). The sodium bicarbonate stock solution was prepared by diluting 48 g sodium bicarbonate in 1 L deionized water (0.57 M). A 0.19 M phosphate buffer solution was prepared by diluting 26.1 g K₂HPO₄ and 5.11 g KH₂PO₄ in 1 L deionized water. All solutions above were stored in the refrigerator at 4 °C before use.

2.2. Acclimation of nitrifying sludge

Activated sludge was taken from aeration tank at Changqiao Wastewater Treatment Plant of Shanghai. Before acclimation, the sludge was washed three times to remove impurities (Zhu et al., 2021a, 2021b). Acclimation was carried in three stages at 30 °C and with a dissolved oxygen (DO) concentration of 6–7 mg/L. For each stage, 700 mL of spent medium was replaced with the same volume of fresh medium daily by pouring supernatant out after settling for 30 min.

The first stage was operated for one week, during which 0.3 g glucose, 1.8 mL ammonium chloride stock (14.6 mgN/L), 5 mL phosphate buffer solution, and 2 mL trace-element solution together with 300 mL sludge were fed into 1 L of medium in cylinder that was aerated. The second stage was operated for ten days, during which the same amount of trace element solution and buffer as the first stage were added, but glucose addition was gradually decreased to zero, while the ammonium chloride stock solution addition was stepwise increased up to 5 mL (about 40 mgN/L). The third stage was operated for one month, during which the amount of trace-element solution and buffer addition was still the same as the second stage, no glucose was added, and the ammonium chloride stock solution addition was still 5 mL (about 40 mgN/L). After the three stages of acclimation, the biomass was highly active in nitrification.

During all following experiments, the acclimated sludge was continuously cultured so that fresh acclimated sludge could be utilized for every experiment.

2.3. Preparation of strain suspension

We cultured two bacterial strains that our group had enriched based on their ability to biodegrade quinoline and its biotransformation products: *Comamonas testosteroni* (MW130858) and *Rhodococcus ruber* (MW433738) (Zhu et al., 2021a, 2021b). Culturing of these strains was carried out in 250-mL conical flask in two stages. All culture processes were operated in thermostatic oscillator at 30 °C and 150 rpm. In the first stage, the two strains were separately inoculated in 100 mL inorganic culture medium from agar-slant-culture-medium, and 3.3 mL quinoline stock was simultaneously added into the medium. After three days, no quinoline was detected, and then the strains were enriched by centrifuging at 8000 rpm for 5 min. In the second stage, the enriched strains were transferred into fresh inorganic culture media separately, and 5 mL of quinoline stock was added into the same volume of fresh medium. After one day, quinoline was no longer detected, and the biomass was settled and further concentrated by centrifugation. The concentrated biomass was then washed three times using sterilized mineral salt medium (Zhu et al., 2021b). Finally, the strains were diluted with the sterilized normal saline to obtain a bacterial suspension with OD₆₀₀ = 1.51 ± 0.05.

2.4. Nitrification and quinoline biodegradation

Experiments to assess nitrification and quinoline biodegradation were carried out in three sets: (1) Acclimated nitrifying sludge was used for nitrification rates with and without quinoline addition. (2) *C. testosteroni* and *R. ruber* were separately added into the acclimated nitrifying sludge to investigate how *C. testosteroni* and *R. ruber* increased nitrification rates in the presence of quinoline. (3) *C. testosteroni* and *R. ruber* were used for biodegradation of 2HQ.

All experiments were carried out in a 250-mL conical flask containing 100 mL of medium. Initial ammonium and quinoline concentrations were 20 mg N/L (1.4 mM) and 32.25 mg/L (0.25 mM), respectively, and the concentration of acclimated nitrifying sludge was 4.5 gDW/L for set (1) and 3.0 gDW/L plus 0.8 gDW/L of *C. testosteroni* or *R. ruber* for set (2). The volume of the bacterial suspension solution was 15% (V/V), corresponding to 0.8 gDW/L in set (3). The conical flasks were put in a thermostatic oscillator at 30 °C, pH 7.8–8.0, and 150 rpm for these experiments, during which samples were taken at one-half hour or one-hour intervals to measure pH, volume, NH₄⁺-N, NO₂⁻-N, NO₃⁻-N, quinoline, and 2HQ. Each experiment was repeated two times. To evaluate if the data were statistically different between the two experiments, we calculated *T* values using the *t*-test (Lu et al., 2019, 2020).

For the three sets of experiments, the acclimated nitrifying sludge was washed with tap water every time before the next experiment to remove nitrate or nitrite retained from the preceding experiment. The washing method was the same as for the acclimation of sludge in Section 2.2.

2.5. Comparison of quinoline and 2-hydroxyl quinoline for their toxicity

Different initial concentrations (0.15 mM ~ 1.5 mM) of quinoline and its intermediate, 2HQ, were assayed by the luminescence of *Vibrio qinghaiensis* to compare their toxicity. The assay steps were fully the same as at Yu et al. (2022b) except that nitrobenzene and *o*-aminophenol were replaced with quinoline and 2HQ.

2.6. High-throughput sequencing

After sets (1) and (2) were completed, three samples – the normal nitrifying sludge as control (designated NS), biomass with *C. testosteroni*

added (designated NS_C), and biomass with *R. ruber* added (designated NS_R) – were immediately submitted to Personal Biotechnology Co., Ltd. (Shanghai, China) for high-throughput sequencing. The steps for DNA extraction and sequencing were the same as that was described by Zhu et al. (2021b). The DNA concentration and purity were detected by NanoDrop 2000, and the quality of DNA extract was detected by 1% agarose gel electrophoresis. 515F (5'-GTGCCAGCMGCCGCGTAA-3') and 907R (5'-CCGTC AATTCCTTTTRAGTTT-3') were the upstream and downstream primers for PCR amplification to the variable region of bacterial 16S rRNA gene V3 and V4.

2.7. Analytical methods

All liquid samples were filtered with a 0.22- μm membrane filter before measurement. A HPLC (model: Ultimate 3000, USA) was used for measuring quinoline and 2HQ at a wavelength of 275 nm for quinoline and 254 nm for 2HQ. The reversed-phase column was ZORBAX SB-C18 column (5 μm , 4.6 \times 150 mm, Agilent). The mobile phase was methanol: water (70:30, V/V) with rate of 1 mL/min, and column temperature was the same 30 $^{\circ}\text{C}$. Ammonium, nitrate, and nitrite were measured with an ion chromatograph having a DIONEX ICS-5000 (Dionex, U.S.) column. Biomass was measured by using Ultraviolet Spectrophotometer (Model: UV-2550, SHIMADZU, Japan) at 600 nm wavelength (i.e., OD_{600}). Total organic carbon analyzer (Shimadzu TOC-I CPN, Japan) was used for measurement of Total organic carbon (TOC).

For biomass dry weight, the washed acclimated sludge of 20 mL was fed into a crucible that was dried at 105 $^{\circ}\text{C}$ in oven for 12 h, and then the dried residue was weighted by using electronic balance (model: METTLER, Toledo, OH, USA) after cooling.

3. Results and discussion

3.1. Effect of quinoline on nitrification rates

Top panel of Fig. 1 shows $\text{NH}_4^+\text{-N}$ removal with and without quinoline added. The bottom panel of Fig. 1 shows that $\text{NO}_3^-\text{-N}$ was generated stoichiometrically in parallel with $\text{NH}_4^+\text{-N}$ removal, thus confirming nitrification. Negligible nitrite N was detected, which means that the $\text{NO}_3^-\text{-N}$ generation rates also represented the nitrification rates (Zou et al., 2019, 2020). All $\text{NH}_4^+\text{-N}$ removal rates were fit well by zero-order kinetics, and the biomass-normalized nitrification rate decreased four-fold in the presence of quinoline: 1.2 ($\text{mg N}\cdot(\text{g biomass})^{-1}\cdot\text{h}^{-1}$) for without quinoline added versus 0.3 ($\text{mg N}\cdot(\text{g biomass})^{-1}\cdot\text{h}^{-1}$) with quinoline added.

3.2. *C. testosteroni* and *R. ruber* accelerated nitrification

In order to relieve inhibition, *C. testosteroni* and *R. ruber* (0.8 gDW/L) were separately added into the acclimated sludge (3 g DW/L) together with the medium containing $\text{NH}_4^+\text{-N}$ and quinoline. The results, shown in Fig. 2, demonstrate that the rates of $\text{NH}_4^+\text{-N}$ removal and $\text{NO}_3^-\text{-N}$ generation rates were very small before 1 h for *R. ruber* addition and 3 h for *C. testosteroni* addition. However, nitrification accelerated rapidly after 1 h or 3 h. Biomass-normalized nitrification rates were 1.3 ($\text{mg N}\cdot(\text{g biomass})^{-1}\cdot\text{h}^{-1}$) and 1.9 ($\text{mg N}\cdot(\text{g biomass})^{-1}\cdot\text{h}^{-1}$), corresponding to 0.8 gDW/L of *R. ruber* and *C. testosteroni* added into 3.0 gDW/L of acclimated sludge in the presence of an initial quinoline concentration of 0.25-mM. Comparing the results in Figs. 1 and 2, the normalized nitrification rates were respectively 4.3- and 6.3-fold greater for additions of *R. ruber* and

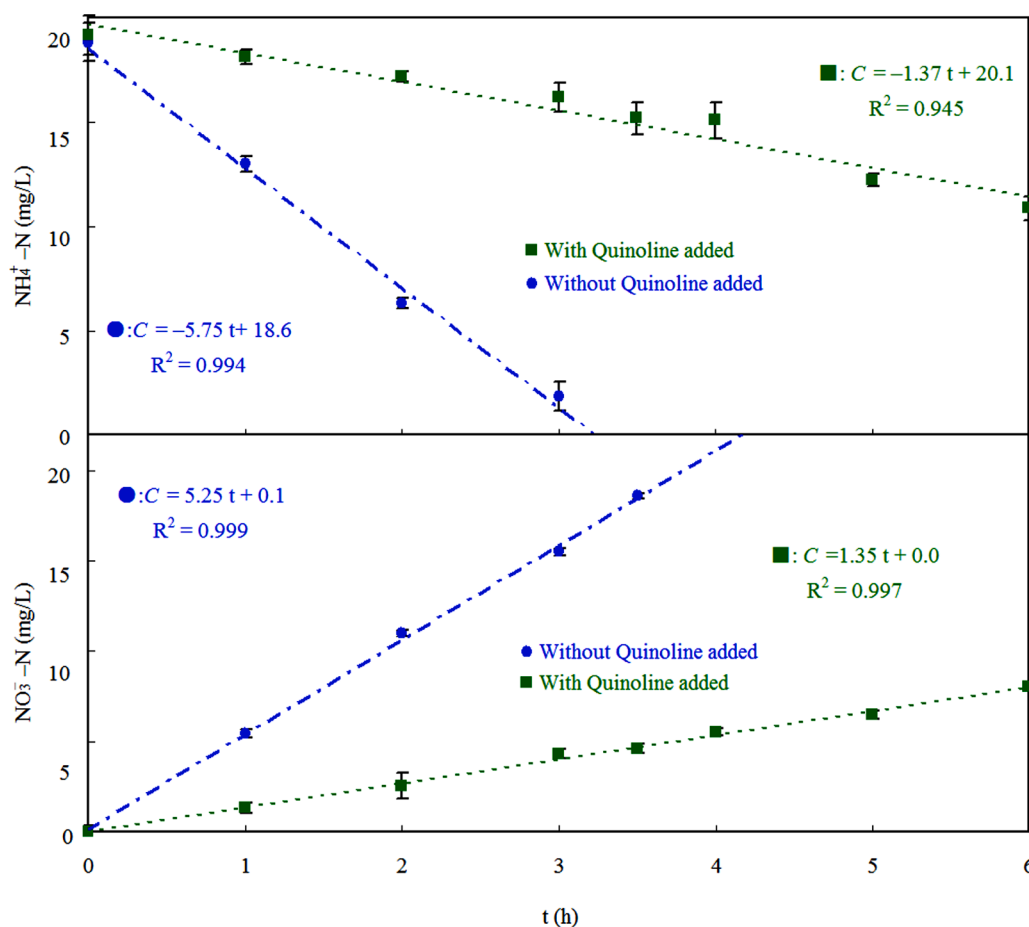


Fig. 1. Comparison of nitrification rates with and without the presence of quinoline. Nitrite is not shown, because it was not detected. The biomass concentrations in the experiments were 4.5 g DW/L. Error bars indicate the range values for the duplicate experiments.

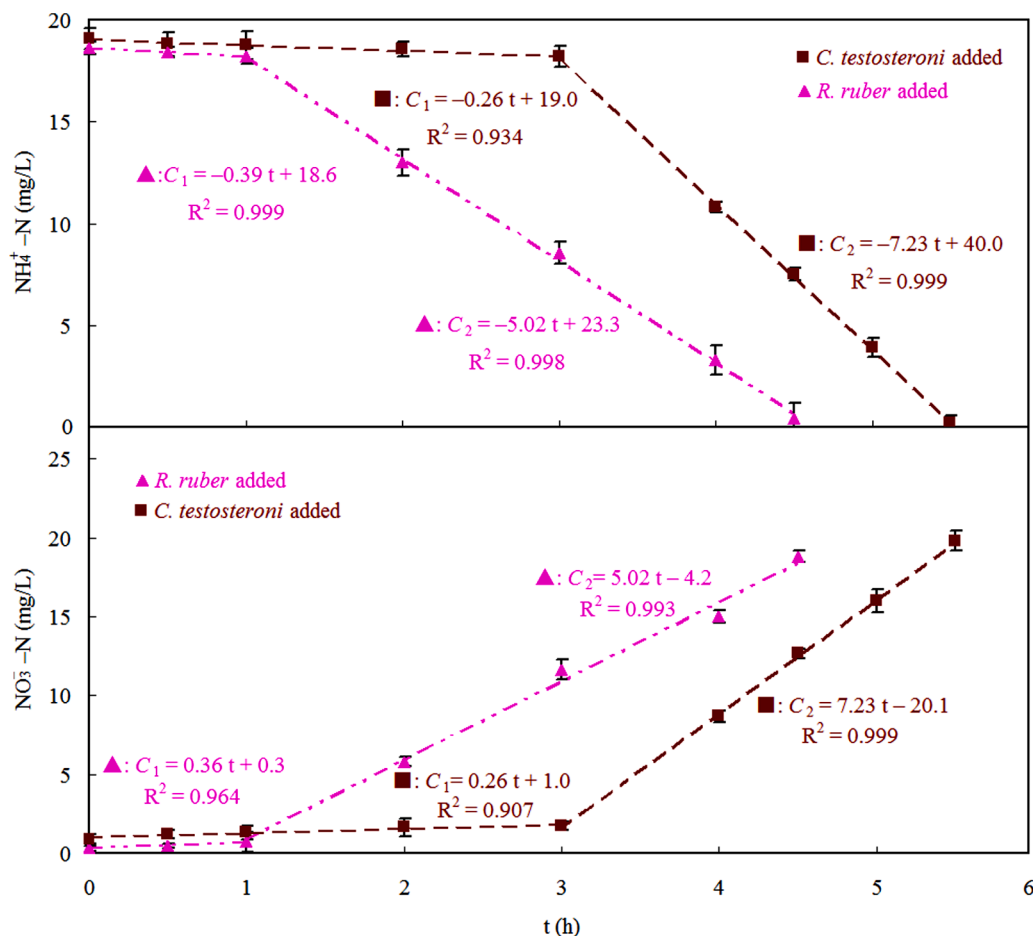


Fig. 2. Effects of adding *C. testosteroni* or *R. ruber* on nitrification in the presence of quinoline. Nitrite is not shown, because it was not detected. The biomass concentrations in the experiments were 3.8 g DW/L. Error bars indicate the range values for the duplicate experiments.

C. testosteroni in the presence of an initial quinoline concentration of 0.25 mM quinoline. Clearly, *R. ruber* and *C. testosteroni* relieved inhibition from quinoline.

The results of Fig. 3 explain why addition of *R. ruber* or *C. testosteroni* relieved inhibition. Quinoline added into the medium was completely biodegraded within 1.5 h in both cases; the zero-order kinetics of quinoline removal was the same for both: 0.16 mM/h. However, the intermediate 2HQ had different fates. With *R. ruber*, 2HQ accumulated to only about 0.025 mM in the first 0.5 h, and it disappeared by 1 h. In contrast for *C. testosteroni* addition, 2HQ accumulated up to 0.2 mM at 1 to 1.5 h before disappearing by 3 h. This shows that the kinetics of the second mono-oxygenation reaction in quinoline biodegradation (Fig. S1) (Bai et al., 2015) were faster than the kinetics of the first mono-oxygenation reaction when *R. ruber* was present. This raises the hypothesis that the relevant functional genes were different between *R. ruber* and *C. testosteroni*. Comparing Fig. 2 with Fig. 3 makes it clear that nitrification did not accelerate until 2HQ disappeared completely; this implies that the inhibition of nitrification was more closely linked to 2HQ than to quinoline.

Fig. S2 in Supporting Information shows that addition of *R. ruber* led to 79% removal of total organic carbon (TOC) in 2 h, compared to 71% removal for *C. testosteroni* addition and 13% removal with no addition. Thus, the TOC removals support that *R. ruber* was more effective at mineralizing added quinoline, which requires that 2HQ be oxidized by the second mono-oxygenation reaction (Fig. S1).

3.3. Comparison of quinoline and 2HQ inhibitions

Fig. 4 shows how increasing concentrations of quinoline and 2HQ increased inhibition to *V. qinghaiensis* sp. (Li et al., 2017; Yu et al., 2022a). 2HQ had stronger inhibition, particularly for the low-concentration range. The inhibition with *V. qinghaiensis* results are consistent with 2HQ having stronger inhibition to nitrifying bacteria.

3.4. Rates of 2HQ biodegradation

R. ruber and *C. testosteroni* were evaluated for their ability to biodegrade 2HQ. As shown in Fig. 5, *R. ruber* was superior to *C. testosteroni* for 2HQ biodegradation: *R. ruber* had a 2HQ-removal rate that was 56% faster than with *C. testosteroni*. This supports why 2HQ disappeared within 1 h for *R. ruber*, but took 3 h for *C. testosteroni* (Fig. 3).

All calculated T values of Figs. 1–5 were larger than $t_{0.005(2)} = 9.9248$, which means that bioaugmentation led to faster rates with a confidence level of 99.5%.

3.5. Microbial communities in the nitrifying biomass

Fig. 6 presents the abundances for top 25 bacterial genera (unique 16S rDNA sequences) for NS (nitrifying sludge), NS_C (nitrifying sludge plus *C. testosteroni*) and NS_R (nitrifying sludge plus *R. ruber*). For sample NS, *Comamonas* and *Rhodococcus* were only 0.5% and 0.2%, respectively, but *Comamonas* increased to 12.0% in NS_C and *Rhodococcus* to 5.9% in NS_R, due to their additions. *Comamonas* also increased in NS_R (3.9%), and *Rhodococcus* increased to 5.5% in NS_C. The best

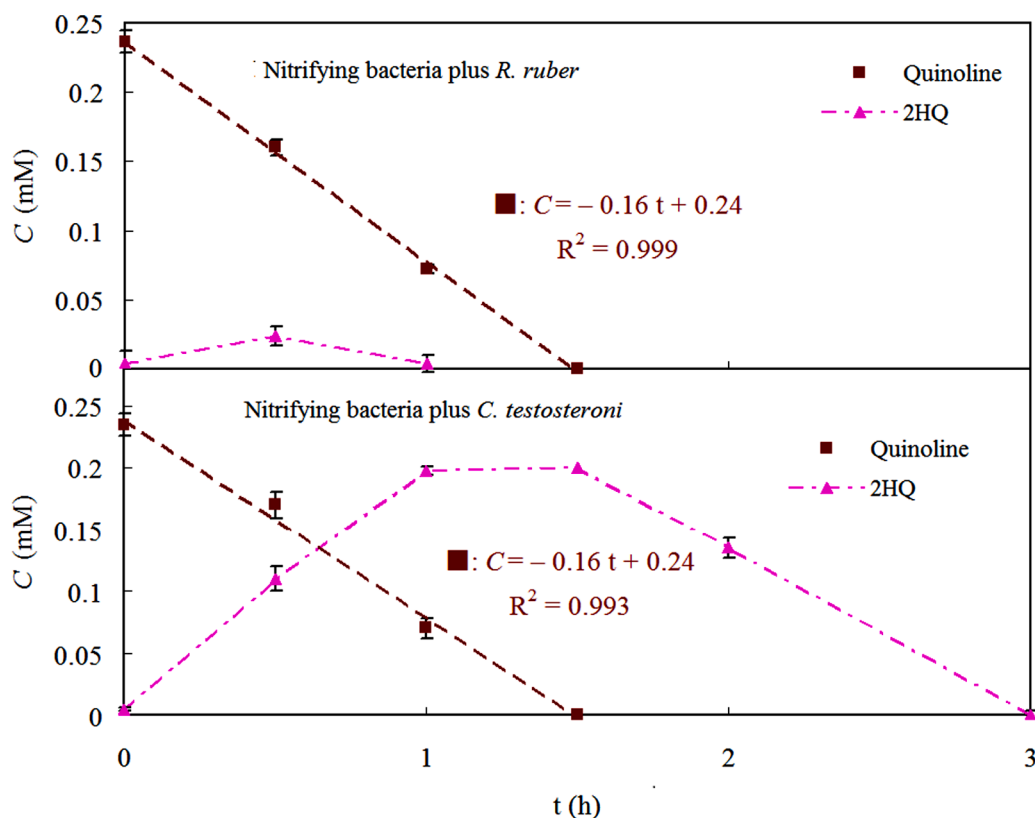


Fig. 3. Fate of quinoline during nitrification. Error bars indicate the range of inhibition for duplicate experiments. Error bars indicate the range values for the duplicate experiments.

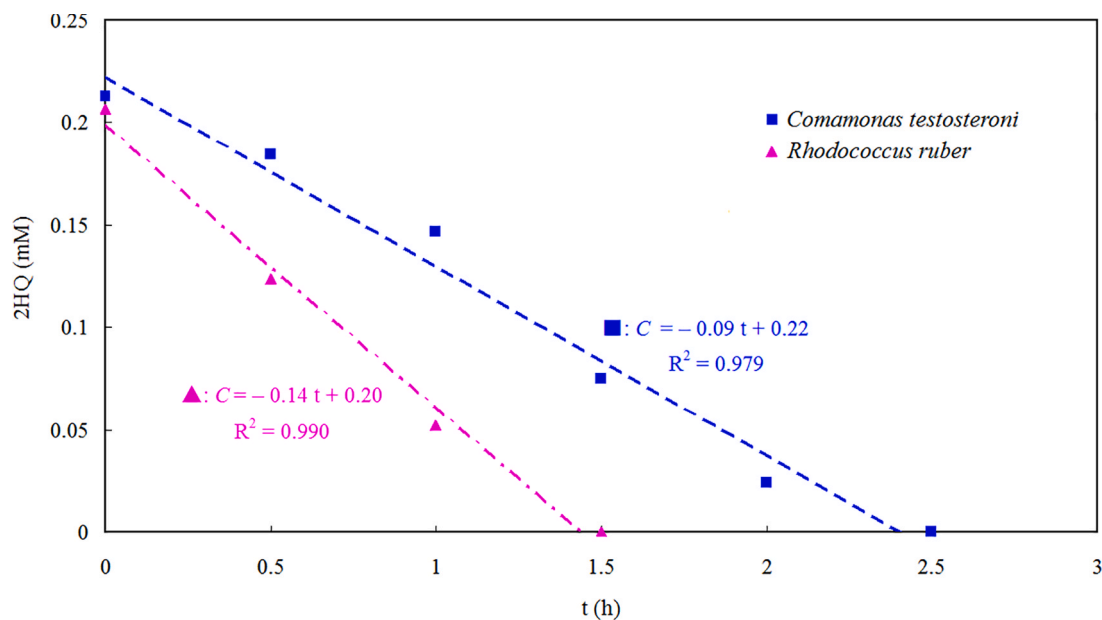


Fig. 4. The inhibitory effects of quinoline and 2HQ on *V. qinghaiensis* as functions of their initial concentrations. Error bars indicate the range values for duplicate experiments.

explanation for this phenomenon is that *C. testosteroni* or *R. ruber* created an improved environment for *Rhodococcus* and *Comamonas* by relieving inhibition to them. Alternatively, it has been reported that *Rhodococcus* was associated with nitrification and denitrification, since nitrate and nitrite generated with ammonium oxidation disappeared (Chen et al., 2012; Wang et al., 2022). However, nitrate generation was equal to

ammonium loss, which indicates that denitrification was not active. In addition, *Rhodococcus* played an important role in biodegrading quinoline intermediates (as shown in Fig. S1 of SI), such as 2,8-dihydroxyl quinoline (Zhu et al., 2008), which can explain why 2HQ accumulated less for NS_R than NS_C (Fig. 3), because abundance of *Rhodococcus* in NS_R was higher than that in NS_C.

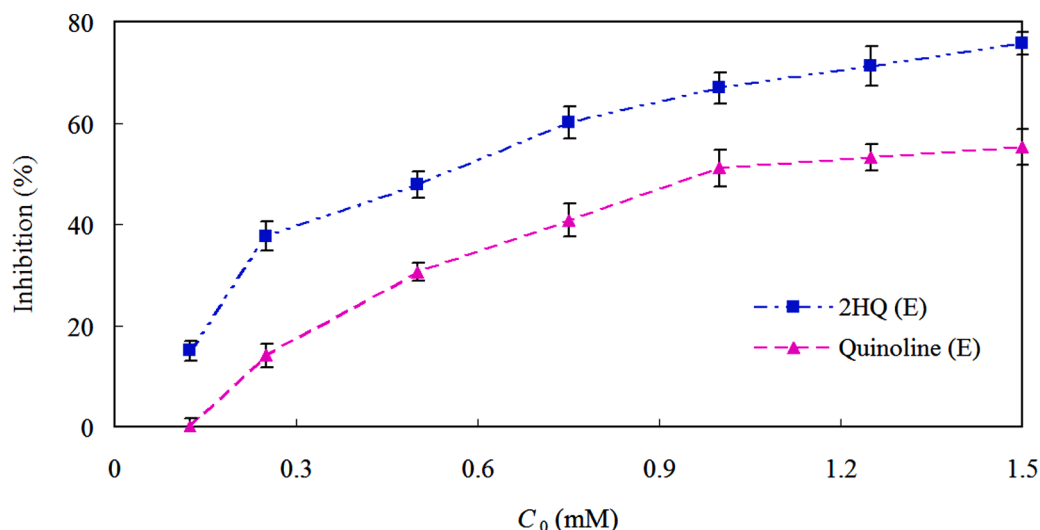


Fig. 5. 2HQ biodegradation with *C. testosteroni* or *R. ruber*. Error bars indicate the range values for the duplicate experiments.

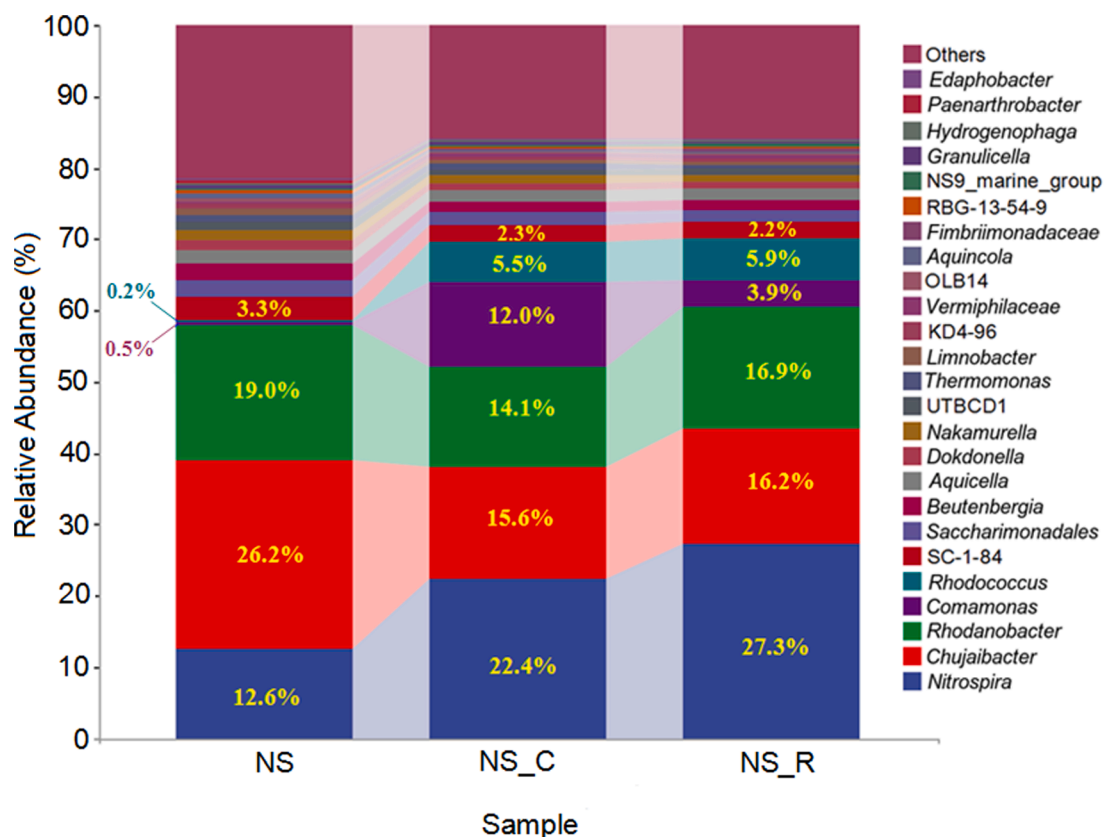


Fig. 6. Top 25 dominant genera in the NS (nitrifying sludge), NS_C (nitrifying sludge plus *C. testosteroni*) and NS_R (nitrifying sludge plus *R. ruber*) at the end of the kinetics experiments. Others contain strains comprising less than 0.2% relative abundance in any of the three systems.

The nitrite-oxidizing genus *Nitrospira* (Al-Ajeel et al., 2022) was important in NS (12.6%), but increased substantially with relief of inhibition in NS_C (22.4%) and NS_R (27.3%). These trends further support that *C. testosteroni* and *R. ruber* relieved the inhibition from quinoline and (especially) 2HQ to nitrification. That *Nitrospira* increased more for *R. ruber* addition than *C. testosteroni* addition is consistent with *R. ruber* being better at relieving inhibition.

Clearly, ammonium oxidation to nitrite was occurring, as nitrate production equaled ammonium loss. However, known ammonium-oxidizing bacteria were not present among the 25 dominant species in

NS, NS_C, or NS_R, even though nitrification kinetics and the abundance of *Nitrospira* increased in NS_C and NS_R. The most likely reason is that *Nitrospira* was carrying out commamox (combined ammonium and nitrite oxidation) (Daims et al., 2015; Al-Ajeel et al., 2022).

Genera *Chujaibacter* and *Rhodanobacter* were highly abundant in NS, but declined in NS_C and NS_R. *Chujaibacter* was important in soils contaminated with polyfluoroalkyl substances (PFAS) and showed a significant positive correlation with PFAS concentrations (Senevirathna et al., 2022). The chemical structure of PFAS is different from quinoline, which suggests that *Chujaibacter* was not involved quinoline

biodegradation. Wu et al. (2022) reported that the genus *Chujaibacter* has potential for lindane degradation. However, lindane also is structurally different from quinoline. The most likely explanation for the relative declines in *Chujaibacter* is that *R. ruber* or *C. testosteroni* became more abundant.

Rhodanobacter existed in soils containing veterinary antibiotics (VAs) and heavy metals (Zhang et al., 2022). Huang et al. (2019) found that *Rhodanobacter* co-existed in a membrane biofilm reactor (MBfR) together with other genera that had functions for oxidizing Hg⁰, nitrification, and denitrification. The relative abundance of *Rhodanobacter* did not change greatly after *C. testosteroni* or *R. ruber* addition, which suggests that *Rhodanobacter* was not involved quinoline biodegradation.

4. Conclusion

Nitrification was inhibited in the presence of quinoline, but the inhibition could be relieved by adding *C. testosteroni* or *R. ruber* to the acclimated nitrifying biomass. Several types of evidence showed that the main inhibitor was 2HQ, the first product of quinoline mono-oxygenation, not quinoline. Thus, rapid biotransformation of 2HQ by a second mono-oxygenation reaction was the key to relieving inhibition, and *R. ruber* was superior to *C. testosteroni* for the second mono-oxygenation. Analysis of microbiological communities showed that abundance of *Comamonas* and *Rhodococcus* increased after *C. testosteroni* or *R. ruber* was added into NS, which created an environment favorable for nitrification. Only one nitrifying genus – *Nitrospira* – had high abundance and increased with addition of *R. ruber* or *C. testosteroni*, which suggests that *Nitrospira* was carrying out commammox metabolism.

Declaration of Competing Interest

The authors declare that they have no known competing financial interests or personal relationships that could have appeared to influence the work reported in this paper.

Acknowledgments

The authors acknowledge the financial support of Special Fund of State Key Joint Laboratory of Environment Simulation and Pollution Control (16K10ESPCT) and Shanghai Youth Teacher Training Program (ZZssd20039).

Supplementary materials

Supplementary material associated with this article can be found, in the online version, at doi:10.1016/j.watres.2022.119455.

References

- Al-Ajeel, S., Spasov, E., Sauder, L.A., McKnight, M.M., Neufeld, J.D., 2022. Ammonia-oxidizing archaea and complete ammonia-oxidizing *Nitrospira* in water treatment systems. *Water Res.* X 15, 100131. <https://doi.org/10.1016/j.wroa.2022.100131>.
- Bai, Q., Yang, L., Li, R., Chen, B., Zhang, L., Zhang, Y., Rittmann, B.E., 2015. Accelerating quinoline biodegradation and oxidation with endogenous electron donors. *Environ. Sci. Technol.* 49 (19), 11536–11542. <https://doi.org/10.1021/acs.est.5b03293>. DOI.
- Chaali, M., Ortiz, H.A.R., Cano, B.D., Brar, S.K., Ramirez, A.A., Arriaga, S., Heitz, M., 2021. Immobilization of nitrifying bacteria on composite based on polymers and eggshells for nitrate production. *J. Biosci. Bioeng.* 131 (6), 663–670. <https://doi.org/10.1016/j.jbiosc.2021.01.010>.
- Chen, P., Li, J., Li, Q.X., Wang, Y., Li, S., Ren, T., Wang, L., 2012. Simultaneous heterotrophic nitrification and aerobic denitrification by bacterium *Rhodococcus* sp. CPZ24. *Bioresour. Technol.* 116, 266–270. <https://doi.org/10.1016/j.biortech.2012.02.050>.
- Daims, H., Lebedeva, E.V., Pjevac, P., Han, P., Herbold, C., Albertsen, M., Jehmlich, N., Palatinszky, M., Vierheilig, J., Bulaev, A., Kirkegaard, R.H., von Bergen, M., Rattai, T., Bendinger, B., Nielsen, P.H., Wagner, M., 2015. Complete nitrification by *Nitrospira* bacteria. *Nature* 528, 504–550. <https://doi.org/10.1038/nature16461>.
- Deng, M., Zhang, Y., Quan, X., Na, C.H., Chen, S., Liu, W., Han, S.P., Masunaga, S., 2017. Acute toxicity reduction and toxicity identification in pigment-contaminated wastewater during anaerobic-anoxic-oxic (A/A/O) treatment process. *Chemosphere* 168, 1285–1292. <https://doi.org/10.1016/j.chemosphere.2016.11.144>.
- Drewnowski, J., Shourjeh, M.S., Kowal, P., Cel, W., 2021. Modelling AOB-NOB competition in shortcut nitrification compared with conventional nitrification-denitrification process. *J. Phys. Conference Series* 1736, 012046. <https://doi.org/10.1088/1742-6596/1736/1/012046>.
- Felczak, A., Bernat, P., Różalska, S., Lisowska, K., 2016. Quinoline biodegradation by filamentous fungus *Cunninghamella elegans* and adaptive modifications of the fungal membrane composition. *Environ. Sci. Pollut. Res. Int.* 23 (9), 8872–8880. <https://doi.org/10.1007/s11356-016-6116-4>.
- Huang, Z., Wei, Z., Xiao, X., Tang, M., Li, B., Zhang, X., 2019. Nitrification/denitrification shaped the mercury-oxidizing microbial community for simultaneous Hg⁰ and NO removal. *Bioresour. Technol.* 274, 18–24. <https://doi.org/10.1016/j.biortech.2018.11.069>.
- Li, T., Liu, S.-S., Qu, R., Liu, H.-L., 2017. Global concentration additivity and prediction of mixture toxicities, taking nitrobenzene derivatives as an example. *Ecotoxicol. Environ. Saf.* 144, 475–481. <https://doi.org/10.1016/j.ecoenv.2017.06.044>.
- Lu, Q., Zhang, Y., Li, N., Tang, Y., Zhang, C., Wang, W., Zhou, J., Chen, F., Rittmann, B.E., 2020. Using ultrasonic treated sludge to accelerate pyridine and p-nitrophenol biodegradation. *Int. Biodeterior. Biodegradation* 153, 105051. <https://doi.org/10.1016/j.ibiod.2020.105051>.
- Lu, Q., Zhang, C., Wang, W., Yuan, B., Zhang, Y., Rittmann, B.E., 2019. Bioavailable electron donors leached from leaves accelerate biodegradation of pyridine and quinoline. *Sci. Total Environ.* 654, 473. <https://doi.org/10.1016/j.scitotenv.2018.11.129>, 201947.
- Lyu, Y., Ye, H., Zhao, Z., Tian, J., Chen, L., 2020. Exploring the cost of wastewater treatment in a chemical industrial Park: model development and application. *Resour. Conserv. Recycl.* 155, 104663. <https://doi.org/10.1016/j.resconrec.2019.104663>.
- Rochmah, W.N., Mangkoedihardjo, S., 2020. Toxicity effects of organic substances on nitrification efficiency. *IOP Conference Series Earth and Environ. Sci.* 506, 012011. <https://doi.org/10.1088/1755-1315/506/1/012011>.
- Rittmann, B.E., McCarty, P.L., 2020. *Environmental Biotechnology: Principles and Applications*, 2nd ed. McGraw-Hill Book Co, New York.
- Senevirathna, S.T.M.L.D., Krishna, K.C.B., Mahinroosta, R., Sathasivan, A., 2022. Comparative characterization of microbial communities that inhabit PFAS-rich contaminated sites: a case-control study. *J. Hazard. Mater.* 423, 126941. <https://doi.org/10.1016/j.jhazmat.2021.126941>.
- Sterngren, A.E., Sara, H., Per, B., 2020. Archaeal ammonia oxidizers dominate in numbers, but bacteria drive gross nitrification in n-amended grassland soil. *Front. Microbiol.* 6, 1350. <https://doi.org/10.3389/fmicb.2015.01350>.
- Suszek-Opatka, B., Maliszewska-Kordybach, B., Klimkowicz-Pawlas, A., Smreczak, B., 2016. Influence of temperature on phenanthrene toxicity towards nitrifying bacteria in three soils with different properties. *Environ. Pollut.* 216, 911–918. <https://doi.org/10.1016/j.envpol.2016.06.066>.
- Tong, N., Yuan, J., Xu, H., Huang, S., Sun, C., Wen, X., Zhang, Y., 2019. Effects of 2,4,6-trichlorophenol on simultaneous nitrification and denitrification: performance, possible degradation pathway and bacterial community structure. *Bioresour. Technol.* 290, 121757. <https://doi.org/10.1016/j.biortech.2019.121757>.
- Wang, J., Chen, P., Li, S., Zheng, X., Zhang, C., Zhao, W., 2022. Mutagenesis of high-efficiency heterotrophic nitrifying-aerobic denitrifying bacterium *Rhodococcus* sp. strain CPZ 24. *Bioresour. Technol.* 361, 127692. <https://doi.org/10.1016/j.biortech.2022.127692>.
- Wu, S.C., Chang, B.S., Li, Y.Y., 2022. Effect of the coexistence of endosulfan on the lindane biodegradation by *Novosphingobium barchaimii* and microbial enrichment cultures. *Chemosphere* 297, 134063. <https://doi.org/10.1016/j.chemosphere.2022.134063>.
- Xu, H., Sun, W., Yan, N., Li, D., Wang, X., Yu, T., Zhang, Y., Rittmann, B.E., 2017. Competition for electrons between pyridine and quinoline during their simultaneous biodegradation. *Environ. Sci. Pollut. Res. Int.* 24 (32), 25082–25091. <https://doi.org/10.1007/s11356-017-0082-3>.
- Yu, Q., Duan, X., Gu, Y., Li, J., Zhang, X., Chen, C., Zhao, D., 2022a. Increasing chemical oxygen demand and nitrogen removal efficiencies of surface-flow constructed wetlands in macrophyte-dominant seasons by adding artificial macrophytes. *Bioresour. Technol.* 348, 126755. <https://doi.org/10.1016/j.biortech.2022.126755>.
- Yu, X., Zhu, G., Gao, Y., Wu, Z., Zhang, P., Zhang, X., Qian, C., Chen, F., Zhang, Y., Liu, R., Rittmann, B.E., 2022b. Roles of *Pseudomonas aeruginosa* and *Ensifer adhaerens* in accelerating nitrobenzene biodegradation by removing an inhibitory intermediate. *Int. Biodeterior. Biodegradation* 171, 105419. <https://doi.org/10.1016/j.ibiod.2022.105419>.
- Zhang, C., Yan, N., Zhu, G., Chen, F., Yu, X., Huang, Z., Zhang, Y., Rittmann, B.E., 2021. Recovery of the nitrifying ability of acclimated biomass exposed to para-nitrophenol. *Sci. Total Environ.* 781, 146697. <https://doi.org/10.1016/j.scitotenv.2021.146697>.
- Zhang, X., Gong, Z., Allinson, G., Li, X., Jia, C., 2022. Joint effects of bacterium and biochar in remediation of antibiotic-heavy metal contaminated soil and responses of resistance gene and microbial community. *Chemosphere* 299, 134333. <https://doi.org/10.1016/j.chemosphere.2022.134333>.
- Zhu, G., Xing, F., Tao, J., Chen, S., Li, K., Cao, L., Yan, N., Zhang, Y., Rittmann, B.E., 2021a. Synergy of strains that accelerate biodegradation of pyridine and quinoline. *Environ. Manage.* 285, 112119. <https://doi.org/10.1016/j.jenvman.2021.112119>.
- Zhu, G., Zhang, Y., Chen, S., Wang, L., Zhang, Z., Rittmann, B.E., 2021b. How bioaugmentation with *Comamonas testosteroni* accelerates pyridine mono-oxygenation and mineralization. *Environ. Res.* 193, 110553. <https://doi.org/10.1016/j.envres.2020.110553>.

Zhu, S., Liu, D., Fan, L., Ni, J., 2008. Degradation of quinoline by *Rhodococcus* sp. QL2 isolated from activated sludge. *J. Hazard. Mater.* 160, 289–294. <https://doi.org/10.1016/j.jhazmat.2008.02.112>.

Zou, S., Yan, N., Zhang, C., Zhou, Y., Wu, X., Wang, J., Liu, Y., Zhang, Y., Rittmann, B.E., 2019. Acclimation of nitrifying biomass to phenol leads to persistent resistance to

inhibition. *Sci. Total Environ.* 693, 133622 <https://doi.org/10.1016/j.scitotenv.2019.133622>.

Zou, S., Zhang, Y., Chen, F., Yu, X., Wu, X., Zhang, C., Rittmann, B.E., 2020. Nitrifying biomass can retain its acclimation to 2,4,6-trichlorophenol. *Water Res.* 185, 116285 <https://doi.org/10.1016/j.watres.2020.116285>.